IEEE/RSJ International Workshop on Intelligent
Robots and Systems IROS '91, Nov. 3-5, 1991,
Osaka, Japan. IEEE Cat. No. 91TH0375-6

Mobile Robot Motion Planning - Stability, Convergence and Control

M.D.Adams, P.J.Probert
Robotics Research Group
Department of Engineering Science
Oxford University
U.K.

Abstract

This paper presents a unified approach to the navigation and control of a mobile robot. In the past, path planning has often been referred to as a "high level" task and has been completely separated from the so called "lower level" control of a real mobile vehicle. We consider here the total energy of a mobile vehicle when influenced under a goal seeking navigation strategy. This energy function is used to produce a control law directly to drive a mobile vehicle. We also incorporate directly an estimate of an artificial repulsive potential field into the low level controller.

1 Introduction

In recent years, the construction and analysis of exact robot navigation algorithms ie: those which guarantee the safe convergence of the trajectory of a mobile robot from a point of origin to a point of destination, has become a growing concern. In this paper we interrelate a method for the path planning of a mobile robot to the application of a correct control law. We take our inspiration from the work by Daniel E. Koditschek [4], in that we derive a control law for a mobile vehicle from considerations of its total energy, when influenced under the action of a potential field. We explore how far we can use the known theoretical tools of classic and non-linear control theory, to safely manoeuvre a real mobile vehicle within a previously unexplored and unstructured environment. In section 2 we derive a control law for any mobile vehicle placed under the action of both attractive and repulsive artificial potential forces. Contrary to previous work, we incorporate directly an estimate of the repulsive component of the artificial potential field, produced by an on board sensor, into the motor control system driving the robot. This is done in order to allow the real time and continuous calculation of the artificial repulsive force field acting upon the mobile. Section 3 analyses the stability and convergence properties of the closed loop system suggested in section 2. As an addition to previous work we find necessary and sufficient conditions for asymptotic tracking of the target input vectors. The application of the derived control law to real vehicles is discussed in section 4 along with a quantitative analysis of the aforementioned conditions, in terms of a mobile robot's motoring parameters.

2 Control: Energy Considerations

Consider an unknown potential function ψ which assigns a scalar value to every position within the plane surrounding the mobile observed by the sensor, and vanishes uniquely at the target with position vector $\mathbf{x}_d$, ie: $\psi(\mathbf{x}_d) = 0$. With the inclusion of its kinetic energy, the total energy possessed by the robot is η given by:

$$\eta = \frac{1}{2} M \dot{\mathbf{x}}^T \dot{\mathbf{x}} + \psi \tag{1}$$

where M represents the total mass of the mobile and $\dot{\mathbf{x}}$ its velocity vector within the plane. Differentiation with respect to $\mathbf{x}$ of η, gives the total external force acting on the mobile robot:

$$\mathbf{F}_{ext} = \frac{\partial \eta}{\partial \mathbf{x}} = M\ddot{\mathbf{x}} + \nabla\psi \tag{2}$$

In equation 2, $\nabla\psi$ is the *total force function* which is perpendicular to ψ at all points in space.

We consider the potential function to be made up of two components, namely an attractive field ψ_{att}, and a repulsive field ψ_{rep}. The attractive field or "cost function" assigns scalar values, within the plane of action of the mobile, which vanish uniquely at the target $\mathbf{x}_d$ and grow larger farther away from $\mathbf{x}_d$. A simple example of this is the quadratic Hooke's Law function:

$$\psi_{att} = \frac{1}{2} K_1 (\mathbf{x} - \mathbf{x}_d)^2 \tag{3}$$

In order to find the total external force on the mobile, we need the value of $\nabla\psi$ to enter into equation 2, so by using equation 3 we obtain:

$$\nabla\psi = K_1(\mathbf{x} - \mathbf{x}_d) - \nabla\psi_{rep} \tag{4}$$

Discrete values of $\nabla\psi_{rep}$ are produced from single distance readings from the centre of our mobile to points within its local environment. After a full 360° rotational scan of the environment produced by the on board sensor, these discrete values are resolved along the components of the two dimensional velocity vector of the robot and summed in order to produce the vector $\nabla\psi_{rep}$ [2].

If we let $\mathbf{F}_{ext}$ in equation 2 represent a dissipative force:

$$\mathbf{F}_{ext} = -K_2\,\dot{\mathbf{x}} \tag{5}$$

the negative sign indicating *dissipation*, $\dot{\mathbf{x}}$ the velocity vector of the mobile and K_2 a positive constant, then as the mobile pursues its goal, its total energy must decrease for all non-zero velocity states.

By substituting for $\nabla\psi$ (equation 4) and $\mathbf{F}_{ext}$ (equation 5) and using the substitution $s = \frac{\partial}{\partial t}$ within the equilibrium force equation 2, we arrive at the result:

$$\dot{\mathbf{x}} = \frac{K_1}{K_2}[\mathbf{x}_d - (1 + s^2\frac{M}{K_1})\mathbf{x} + \frac{1}{K_1}\nabla\psi_{rep}] \quad (6)$$

Hence by considering the total energy of a mobile, when under the influence of an artificial potential field, we have arrived at a possible control law, namely that the desired velocity signal to the motors should be dependent upon both position and acceleration feedback of the robot.

We note also that if a motor produces a torque $\mathbf{T} = rM\ddot{\mathbf{x}}$ where r is the radius of the driving wheels and M the mass of the vehicle carried by each wheel, then:

$$\mathbf{T} = rK_1[\mathbf{x}_d - (1 + s\frac{K_2}{K_1})\mathbf{x} + \frac{1}{K_1}\nabla\psi_{rep}] \quad (7)$$

Equation 7 shows that if torque control is preferred, then the desired torque signal to the motors should depend upon both the position and *velocity* of the robot.

3 Stability and Convergence

A natural progression on the "possible control law", given in equation 6, is to pose the question: "Can we guarantee stability and hence convergence of the mobile to the desired position vector $\mathbf{x}_d$?" From equations 1 and 3 we can write an expression for the total energy of the mobile robot:

$$\eta = \frac{1}{2}M\dot{\mathbf{x}}^T\dot{\mathbf{x}} + \frac{1}{2}K_1(\mathbf{x} - \mathbf{x}_d)^2 - \psi_{rep} \quad (8)$$

so that its rate of change of energy is given by:

$$\dot{\eta} = -K_2\dot{\mathbf{x}}^T\dot{\mathbf{x}} \quad (9)$$

Hence if the total energy of the mobile is used as a *Lyapunov function* [5], then we can guarantee global asymptotic stability of the mobile with respect to $\mathbf{x}_d$, provided the following conditions are met:

1. *Global Asymptotic Stability :*
   - The net force given by:
   $$M\ddot{\mathbf{x}} + K_1(\mathbf{x} - \mathbf{x}_d) - \nabla\psi_{rep} = -K_2\dot{\mathbf{x}} \quad (10)$$
   is always in the direction of the equilibrium position $\mathbf{x}_d$ so that:
   - The velocity vector $\dot{\mathbf{x}}$ never reaches zero until $\mathbf{x} = \mathbf{x}_d$.
2. *The local minimum of ψ is at $\mathbf{x} = \mathbf{x}_d$.* Upon receipt of a single 360° scan of the local environment accessible by the sensor's infra-red light, we arrange that the attractive force towards $\mathbf{x}_d$ plus the inertial force of the robot is always greater than the repulsive force, $\nabla\psi_{rep}$. We therefore ensure that the target $\mathbf{x}_d$ is a true equilibrium point of ψ as generated by the Hooke's Law cost function and the sensor scan.

The velocity signal $\dot{\mathbf{x}}$ in equation 6 can assume any values, dictated by $\mathbf{x}_d$, $\mathbf{x}$ and $\nabla\psi_{rep}$. In reality of course, a real vehicle cannot travel at any speed and will be limited to $\pm$U m/s say. We can take this into account, by replacing the linear amplifier having gain K_1/K_2, in equation 6, with a non-linear ideal saturation with the same gain but saturation levels of $\pm$U. Examination of equations 8 and 9 will reveal that the total energy is still positive definite and that the rate of increase of energy is still negative definite under the same conditions 1 and 2.

4 Application to Real Vehicles

The energy considerations used thus far have proved extremely useful in providing us with a proven globally asymptotically stable speed controller given in equation 6, provided conditions 1 and 2 are adhered to. It has however provided no insight into the possible numerical values of K_1 and K_2 (other than that they must both be positive). A quantitative analysis of conditions 1 and 2 is necessary to provide these limiting values, and the dependence of condition 1 upon the robot's motor dynamics will be shown here, whilst the quantitative application of condition 2 is left until section 4.4.

After forming the transfer functions for each vehicle (ie: transferring $\dot{\mathbf{x}}$ into $\mathbf{x}$), we will apply the known methods of classical and non-linear control theory in order to find the limiting values for K_1 and K_2. We will firstly determine the general relationship between K_1, K_2 and the distance q of the mobile robot from its target, at which a stable oscillation can occur. In section 4.2, we will use the general result in order to guarantee that no stable limit cycle can occur within a vehicle's control system throughout its entire trajectory. This is necessary because, as stated in condition 1, the mobile's velocity vector $\dot{\mathbf{x}}$ must not reach zero until convergence. Hence oscillations about, or overshoot of, the equilibrium position would be undesirable.

In [1] the general relationship between K_1, K_2 and q is used to purposely produce a small oscillation in order to create a "Self Oscillating Adaptive System" (S.O.A.S). Such a system presents a constant gain to slowly varying signals throughout the loop. This is a useful property since variations of the motor parameters occur with changes in time and temperature, meaning that changes in the gain of the driven process (the motor dynamics) result. [1] shows that an S.O.A.S is capable of automatically changing the gain presented to the slowly varying signals by the non-linearity, in order to maintain an overall constant loop gain, even if the process gain changes. By ensuring that the amplitude of the allowed oscillation is small enough, the motors will be unable to respond to it, implying the possibility of an *adaptive* asymptotically stable system.

Figure 1 shows the full control system derived so far, for any vehicle with its own *speed* controller and approximately linear motor dynamics.

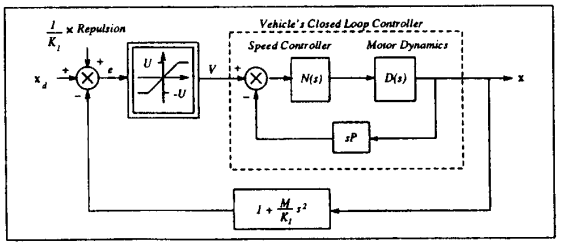

Figure 1: A realistic control system for a permanent magnet d.c motor driven robot, under the influence of an artificial potential field.

To simplify the analysis of the complete control system in figure 1, we replace the closed loop vehicle's speed controller and dynamics with its open loop equivalent $H(s)$ - ie:

$$H(s) = \frac{N(s)D(s)}{1 + sPN(s)D(s)} \tag{11}$$

where $N(s)$ is a vehicle's speed controller, $D(s)$ its motor dynamics and P is its velocity feedback gain. Figure. 2 shows the resulting system.

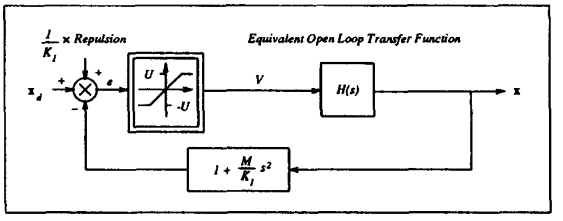

Figure 2: The resulting control system with a mobile robot's speed controller and motor dynamics replaced by their open loop equivalent transfer function $H(s)$.

It has become the general trend of many researchers to use mobile vehicles with on board *proportional, integral, derivative* (P.I.D) speed control systems. The assumption which then often follows is that any form of oscillation, overshoot or instability of a mobile vehicle, when in pursuit of a target, will not occur. Low level control and so called 'high level' path planning has often been separated in this way, in an attempt to remove the burden of a mobile vehicle's motor control theory from the researcher. We will show in the following sections that this assumption is only true under certain conditions, and that full P.I.D control is unnecessary for overall position control, as it does not allow faster convergence (ie: a steeper gradient within the non-linearity) of a mobile to its target. We will further show the necessary and sufficient conditions for stable, asymptotic tracking of a target, to the level of generality of the speed controller $N(s)$ being part or all of a P.I.D system. Results of experiments using one of Oxford's vehicles under the overall position control system in figure 1 will be demonstrated.

4.1 Describing Function Analysis

We now analyse our system to show what quantitative effect condition 1 (page 5) provides. We will show that in order not to obtain a limit cycle within the system (ie: to stop oscillations of the vehicle about a position vector $\mathbf{x}$) there is an upper limit on how large the gradient $\frac{K_1}{K_2}$ of the linear region within the saturation may be. If this gradient is exceeded, an oscillation with a known amplitude and frequency will be observed as the vehicle performs oscillations about the equilibrium point. For each oscillation performed, two reversals of the velocity vector $\dot{\mathbf{x}}$ result meaning that condition 1 is violated. We will further show the effect of the inertial term within the feedback loop of figure 2. This term allows us to increase the gradient $\frac{K_1}{K_2}$ almost to the limiting condition of the non-linearity becoming a perfect relay without observing oscillations, meaning that a mobile vehicle could theoretically track its target at maximum speed until it is reached. This means that the non-linearity could almost supply the motors with time optimal *bang bang* control.

Because the motor dynamics in our control loop are third order, phase plane analysis of the system response is not practical. We therefore use the method of *describing functions* [5]. As the difference in the desired signal $\mathbf{x}_d$, the output $\mathbf{x}$ and any disturbance produced by the on board sensor approaches the steady state (ie: the mobile moves towards convergence), there will be other signals superimposed onto any stable limit cycle oscillations. Therefore the signals appearing at the input of the non-linearity will be of the form:

$$w(t) = a\sin\omega t + q(t) \tag{12}$$

where $a\sin\omega t$ denotes the limit cycle oscillation and $q(t)$ represents the superimposed signals. Since $q(t)$ will primarily be caused by the error signal $(\mathbf{x}_d - \mathbf{x})$, we assume that it varies much slower than $\sin\omega t$ and that it is smaller in magnitude than a which is certainly true near the steady state (when the oscillations occur) as the model and process outputs are similar. Since $q(t)$ varies slowly we approximate it by a constant in the above equation, so that:

$$w(t) \approx a\sin\omega t + q \tag{13}$$

If such a signal existed within our system, then the output of the non-linear saturation would appear as in figure 3b.

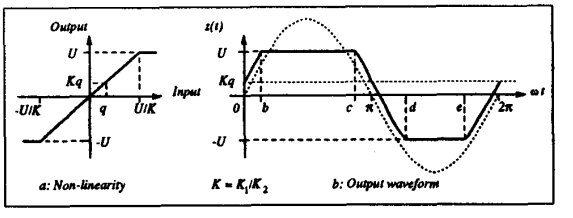

Figure 3: Output waveform produced by the non-linear saturation in response to the signal $w(t) = a\sin\omega t + q$ for $a > \frac{UK_2}{K_1} + q$.

The output waveform can be represented as a Fourier Series:

$$z(t) = N_0 + n_1\sin(\omega t + \phi) + n_2\sin(2\omega t + \phi) + n_3\sin(3\omega t + \phi) + \ldots \tag{14}$$

The non-linearity presents different transfer properties to the oscillation $a\sin\omega t$ and the 'd.c signal' q. To consider the transmission of both signals through the saturation the *dual input describing function* method is necessary [3]. The describing function with which we replace the non-linearity, when considering oscillations, is given by:

$$F(\theta) = \frac{K}{\pi}[\sin^{-1}\theta + \sin^{-1}T\theta + \frac{U\theta}{(U - Kq)}(\cos(\sin^{-1}\theta) + \cos(\sin^{-1}T\theta))] \times (\cos(\sin^{-1}(\frac{q}{a})) + j\frac{q}{a}) \tag{15}$$

which is expressed in terms of the variables a and θ, where $\theta = (U - Kq)/Ka$, $K = \frac{K_1}{K_2}$ and $T = (U + Kq)/(U - Kq)$, in order to simplify the analysis. Under the assumptions made earlier, q/a is small so that we assume $F(\theta)$ and hence $F(a)$ to be approximately real valued.

For the "slowly" varying signal, the gain presented by the non-linearity is approximately given by the dual input describing function:

$$F' = \frac{N_0}{q} \tag{16}$$

where N_0 is the d.c value of $z(t)$ in figure 3.

4.2 Avoiding Limit Cycles

In order to avoid a limit cycle during the complete trajectory of a mobile vehicle the condition:

$$\frac{\pi}{K}[\sin^{-1}(\frac{U-Kq}{U+Kq})+\frac{\pi}{2}+\frac{U}{(U-Kq)}\cos(\sin^{-1}(\frac{U-Kq}{U+Kq}))]^{-1} > \mid G(j\omega_0)\mid \quad (17)$$

must be obeyed for all values of q as $q \rightarrow 0$ (ie: the robot converges).

In equation 17, $\mid G(j\omega_0)\mid$ represents the gain of the closed loop system (not including the non-linearity) at the possible oscillation frequency ω_0, ie: in figure 2:

$$G(j\omega_0) = H(j\omega_0)[1-\frac{M}{K_1}\omega_0^2] \quad (18)$$

4.3 Experimental Results

Experimental results using Oxford's smallest mobile vehicle produced interesting results. The speed controller on the vehicle is an integral one, and the application of equation 17 gives a condition on K_1 and K_2 as $q \rightarrow 0$:

$$(K_1 - A) < BK_2 \quad (19)$$

where A and B are positive constants. It can be seen from the equation that it is theoretically possible to allow K_2 to approach zero (although equation 5 shows that for constant energy dissipation $K_2 > 0$), allowing K_1/K_2 to become large, almost to the limiting condition of the non-linearity becoming a perfect relay. It is also interesting to note that if the inertial term were not present within the feedback loop of figure 1 (ie: simple position feedback only were used), equation 19 would be of the form:

$$K_1 < BK_2 \quad (20)$$

for no oscillations. The effect of the acceleration feedback, derived from the energy considerations, is clear since it allows a much higher loop gain, and hence faster tracking of the input vectors $\mathbf{x}_d$. Figures 4 to 6 show curves of the angle θ of the mobile robot within a plane coordinate system, as it tracks a constant input vector $\mathbf{x}_d$, versus time. For Eric, the motoring parameters show that if an oscillation results, its frequency is constant and the above analysis yields a value $\omega_0 \approx 5.1$ Hz. In figure 4, K_1 and K_2 are allowed to violate equation 19. An oscillation occurs at $q = 0.025$ radians at a frequency of 4.4 Hz and an amplitude of 0.030 radians. By decreasing the gradient K_1/K_2 so that it obeys equation 19, figure 5 results. By decreasing K_2 significantly to just above zero, K_1 is slightly larger than A, so that we allow more acceleration feedback. Hence figure 6 shows the effect of K_1/K_2 being equal to that in figure 4 so that the overall loop gain is the same, but the individual values of K_1 and K_2 now obey equation 19.

4.4 Steady State Analysis

Provided we avoid limit cycles by invoking the above conditions, Lyapunov's theory indicates asymptotic tracking of target vectors $\mathbf{x}_d$. We now apply steady state analysis to the control system of figure 2 to discover the type of input necessary (ie: steps, ramps etc) to yield zero steady state error.

In the steady state, when the transient behaviour of the error

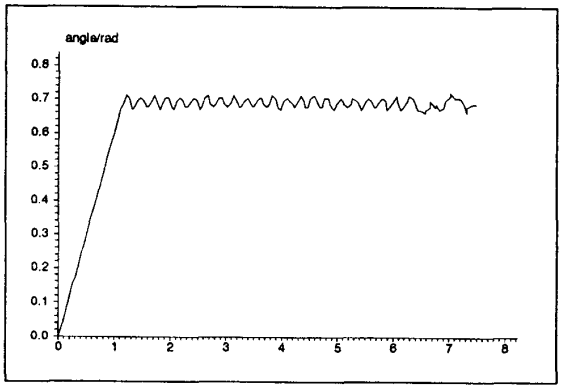

Figure 4: A gain of 1200 within the linear region of the saturation causes an oscillation, because the constant K_1 set to 1200 greatly attenuates the acceleration feedback.

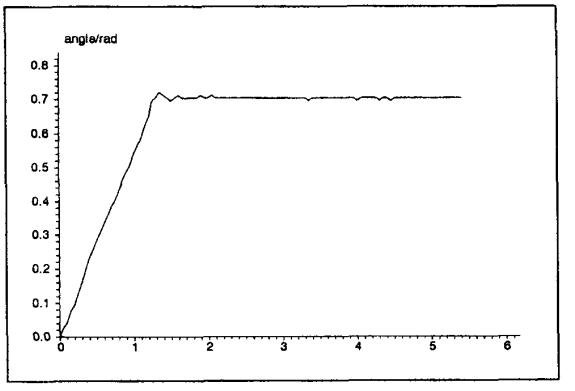

Figure 5: A gain of 500 within the linear region of the saturation causes no oscillation, since both K_1 and K_2 obey the above condition.

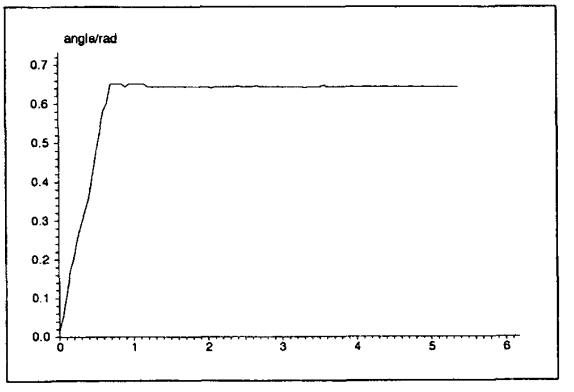

Figure 6: A gain of 1200 within the linear region of the saturation causes no oscillation, since both K_1 and K_2 obey the above condition.

signal e has decayed, we can assume e to be small enough such that the saturation is operating within its linear region. From figure 2:

$$\mathbf{x} = H(s)\frac{K_1}{K_2}e \tag{19}$$

and when the disturbance caused by the repulsive force field, $\nabla\psi_{rep}$ is zero:

$$e = \mathbf{x}_d - (1 + \frac{M}{K_1})s^2\mathbf{x} \tag{20}$$

Therefore:

$$\mathbf{x} = \frac{H(s)\frac{K_1}{K_2}\mathbf{x}_d}{1 + H(s)\frac{K_1}{K_2}(1 + s^2\frac{M}{K_1})} \tag{21}$$

If we let $\mathbf{x}_d$ be a step input, which in the s domain is given by:

$$\mathbf{x}_d = \frac{E}{s} \tag{22}$$

where E is the magnitude of the step, then the steady state error e_{SS} is given by:

$$\lim_{s\to 0} e_{SS} = s(\mathbf{x}_d - \mathbf{x}) = E(1 - \frac{\frac{1}{P}\frac{K_1}{K_2}}{\frac{1}{P}\frac{K_1}{K_2}}) = 0 \tag{23}$$

Hence we can design an algorithm which can inject values for target positions $\mathbf{x}_d$ which the mobile is to pursue. Provided these inputs take the form of steps, we are guaranteed that zero steady state error will result, meaning that the target will be reached.

4.4 Conditioning the Repulsive Field

In accordance with condition 2, we need to determine a value for the attractive force field constant K_1 in order to limit the overall effect of the repulsive force field. Figure 1 shows that the repulsive input to the control system is attenuated by the constant $\frac{1}{K_1}$.

The theoretical *worst case* repulsion possible upon our mobile vehicle is shown by the specific environmental condition in figure 7.

If a mobile were to position itself at the goal G within the environment shown in figure 7, its repulsive force field against its direction of motion would be at its maximum. This is because there is no scenery behind the robot to 'repel' it in its direction of motion.

Upon completion of a 360° scan of the environment, the on board sensor at position G in figure 7 will provide an estimate of $\nabla\psi_{rep}$ given by:

$$\nabla\psi_{rep\,MAX} = \frac{1}{R^2} + \frac{2}{R^2}\sum_{i=1}^{(\pi/2\gamma)}\cos(i\gamma) \tag{21}$$

where γ = sensor incrementing angle, R is the smallest allowable distance between the centre of the robot and a point in the environment as shown in figure 7 and i is an integer.

By allowing only this maximum repulsive effect to exactly cancel the overall attraction of the mobile to its target, we fulfill condition 2 since a reversal of the vehicle's velocity is not possible. We therefore equate the repulsive input in figure 1 to the maximum value of $\mathbf{x}_d - (1 + \frac{M}{K_1}s^2)\mathbf{x}$ which will just cause saturation at the non-linearity. It can be seen from figure 3 that the input value necessary to just cause saturation is:

$$\text{Input at saturation} = \frac{UK_2}{K_1} \tag{22}$$

so that the above condition is given by:

$$\frac{\nabla\psi_{rep\,MAX}}{K_1} = \frac{UK_2}{K_1} \tag{23}$$

so that:

$$K_2 = \frac{\nabla\psi_{rep\,MAX}}{U} \tag{24}$$

Equations 24 and 17 provide the necessary conditions for global, asymptotic stability of the vehicle with respect to an equilibrium point $\mathbf{x}_d$. They further guarantee that no local minima will be generated since the repulsive component of the artificial potential field has been conditioned as above. This indicates the necessity for an algorithm that will produce subgoals for the mobile to pursue. It is a further requirement that these subgoals are placed in safe and reachable positions, as we no longer rely upon the repulsive force field for navigation but allow it to influence our control system in order to produce smooth paths for the mobile. [2] shows a method for producing such subgoals.

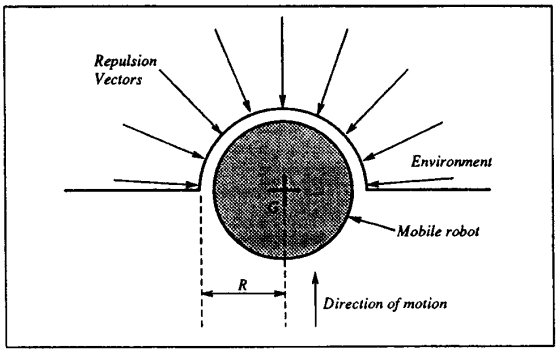

Figure 7: A mobile robot in a position of maximum repulsion from the repulsive component of the artificial potential field. The environment provides repulsion only in a direction opposing the motion of the vehicle.

5 Conclusions

In the past researchers have often treated motion planning and control as separate aspects. In this paper we have presented a unified approach to navigation and control in the form of a proven globally asymptotically stable system, which forces a mobile to track changing targets.

We have further shown a method for overcoming minima within a potential field, provided a goal relocation algorithm is used to provide sub-targets for a mobile to pursue. An estimate of an artificial potential repulsive field is incorporated directly into the mobile's control system, and is provided by an on board infra red time of flight sensor. The mobile test bed used in the experiments is shown in figure 8, carrying such a sensor developed at Oxford. In the near future we intend to apply

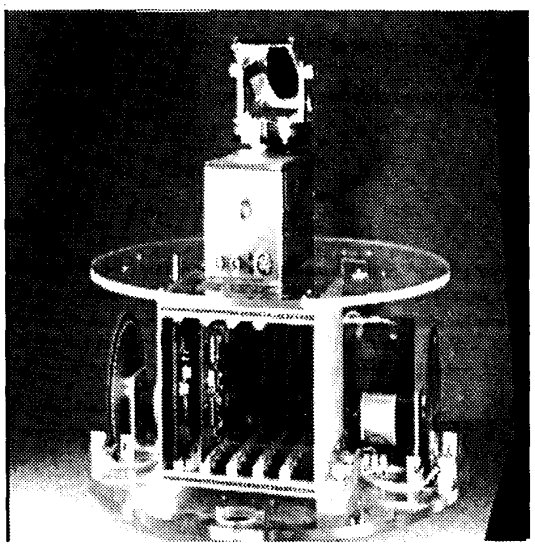

Figure 8: Eric: One of Oxford's mobile robots carrying an infra red time of flight sensor.

the above techniques to other larger vehicles within the lab, in order to study the effect of non-linear motor dynamics upon the proposed navigation strategy.

6 Acknowledgements

We would like to thank Jon Tombs for his help with the software necessary to carry out this work. Martin D Adams is supported by an S.E.R.C grant.

References

[1] Martin D. Adams. Mobile robot navigation and control - phd thesis. Technical report, Oxford U. Robotics Research Group, 1991.

[2] Martin D. Adams and P.J.Probert. Towards a real-time navigation strategy for a mobile robot. In *International Workshop on Intelligent Robots and Systems*, page 743 to 748, 1990.

[3] Karl J. Astrom and Bjorn Wittenmark. *Computer Controlled Systems*. Prentice-Hall, 1987.

[4] Daniel E. Koditschek. *Robot Planning and Control Via Potential Functions - from the Robotics Review*. The M.I.T Press, 1989.

[5] O.L.R.Jacobs. *Introduction to Control Theory*. Clarendon Press, Oxford, U.K, 1974.